ALMA Memo No. 448
UV intensity near AOS and OSF

Seiichi Sakamoto
National Astronomical Observatory of Japan
Mitaka, Tokyo 181-8588, Japan

2003-03-23

Abstract

UV intensity near the AOS and OSF sites in northern Chile was measured with handheld UVA and UVB radiometers and was compared with that taken at Socorro AOC, Nobeyama, and Mitaka. Typical UVA opacity was about 0.4 at Pampa La Bola near the AOS site, about 0.6 both at San Pedro de Atacama near the OSF site and at Nobeyama, and about 0.7 at Mitaka (best conditions), respectively. The UVA intensity toward the Sun measured at Pampa La Bola near the sunset (elevation $\sim 20°$) was still comparable with the highest value recorded at Mitaka. The difference becomes even more outstanding in UVB. The UV Index, which chiefly reflects UVB intensity, measured with a handheld UVB radiometer is in reasonable agreement with that predicted with the satellite data, and both consistently indicate that the UVB is extremely high at the AOS and OSF sites. The UV Index typically exceeds 7 (high) for 6 hours near the AOS site.

1 Introduction

The ALMA site is very dry and high, having a very high millimeter- and submillimeter-wave transparency. In such a site, transparency of ultraviolet light (UV) is also expected to be high. As a result, some of the ALMA instruments, as well as ALMA employees, have potential risks to be overexposed to UV.

The most serious effects of intense UV are those to human health, and these effects have been studied extensively with particular interest in damages of skin and eyes [e.g., 1, 2, 3]. It is well known that human skin is sensitive to UV. Human skin is, however, not equally sensitive to all types of UV[1]. The Erythemal Response Spectrum, a scientific expression that describes human skin sensitivity to UV, has been accepted throughout the world. The Effective UV Spectrum is the mathematical product of the Solar UV Spectrum and the Erythemal Response Spectrum. It can be interpreted as the skin burning intensity of individual wavelengths of sunlight. Although overall sensitivity to sunburning varies among individuals (see, Tables 1, 2), the relative sensitivities to separate wavelengths remain the same.

Intense UV radiation also affects on materials [e.g., 3]. A wide variety of synthetic and naturally-occurring high polymers absorb solar ultraviolet radiation and undergo photolytic, photooxidative, and thermo-oxidative reactions that result in the degradation of the material.

[1]Ultraviolet light is classified into three: UVA in a wavelength range of 320–400 nm, UVB of 290–320 nm, and UVC of 260–290 nm, though the definition seems not very strict. UVA is not absorbed by the ozone layer, while UVB is mostly absorbed by the ozone layer but some reaches the surface. UVB pose the greatest risk of skin cancer. Some UVA is needed by the human body for the synthesis of vitamin D, but excessive amounts cause aging, wrinkling, and loss of elasticity of the skin, and sometimes result in skin cancer and cataracts. UVC is completely absorbed by the ozone layer and oxygen, and is not important as far as solar UV is concerned.

The degradation suffered by these materials can range from mere surface discoloration affecting the aesthetic appeal of a product to extensive loss of mechanical properties that severely limit its performance. The deleterious effects of solar UVB radiation in particular, on wood, paper, biopolymers and polymers (plastics and rubber), are well known. The phenomenon is of special interest to the building industry which relies on polymer building products that are routinely exposed to sunlight during use. Most of the common polymers used in such applications contain photostabilizers to control photodamage and to ensure acceptable lifetimes under outdoor exposure conditions.

Because significant fraction of the ALMA employees and the instruments will stay outdoors at the Chilean sites, appropriate care should be taken by assessing the UV intensity at the site. To examine the UV (both UVA and UVB) intensity near the Array Operations Site (hereafter AOS) and Operations Support Facilities (hereafter OSF) sites as a follow-up of the previous measurements [4], we measured the UV intensity at Pampa La Bola (alt. = 4800 m; near the AOS site) and San Pedro de Atacama (alt. = 2450 m; near the OSF site). Results of the similar measurements at Mitaka (alt. = 60 m, only under best conditions), Nobeyama (alt. = 1350 m), and Socorro AOC (alt. = 1400 m) are also reported for comparison.

2 Measurements

2.1 UVA measurements

Measurements of ground-level UVA intensity were carried out at Pampa La Bola (near the AOS) and San Pedro de Atacama (near the OSF) during the periods of January 18–21, February 27–March 15, April 5, and October 26–November 2, 2002. Ushio UIT-101 radiometer incorporated with Ushio UVD-365PD sensor was used to record the UV intensity. The sensor had a sensitivity range from 330 nm to 390 nm (a part of UVA) with a typical sensitivity curve illustrated in Figure 1 (Ushio Inc. 2001, private communication). The radiometer was calibrated with the 1 mm^2-aperture sensor so that its direct readout for 365 nm monochromatic light provides an intensity with specified absolute calibration error of $< 5\%$ and non-linearity of $< 1\%$. Specified minimum sensitivity of the sensor was $0.01\,\mathrm{mW\,cm^{-2}}$. Because we measured sunlight instead of monochromatic light, the readout should be taken as in arbitrary unit. Because two sets of Ushio UIT-101 + UVD-365PD were used for the two runs, the value for the first run was scaled by 0.87, the factor obtained by side-by-side calibration at Mitaka during February 14–22, 2002.

We measured three positions of the sky: one toward the Sun with and without direct illumination by the Sun (I^{+}_{sun}, I^{-}_{sun}), another toward the zenith with and without direct illumination by the Sun (I^{+}_{zen}, I^{-}_{zen}), and the other toward the horizon in the opposite direction to the Sun (I_{hor}). UV intensity of uniformly-distributed component was evaluated by the data without direct illumination by the Sun. Solar elevation was calculated from the observing time and location coordinates with the Solar Position Calculator [5] provided online by NOAA.

Reference data were collected at Socorro AOC (during January 24–25, 2002), Nobeyama (during February 13 and August 11–13, 2002), and Mitaka (during January 28–February 22, June 19, and July 26–August 9, 2002, and March 20–21, 2003) through similar measurements.

We additionally took a few data toward the ground to evaluate the ground reflectivity in UV wavelengths.

2.2 UVB measurements

Ground-level UVB intensity was measured with SafeSun Classic personal UV radiometer [6]. The sensor had a sensitivity curve quite similar to the Erythemal Response Spectrum as illustrated in Figure 2 and provided a direct readout of the UV Index (UVI)[2] up to UVI = 15 with specified absolute calibration error of less than 20% for UVI < 3 and less than 10% for UVI > 3. The data suffer relatively large effect of quantization errors when the readout is small.

The measurements were carried out in a manner similar to those of UVA intensity described in the above subsection. The data were collected at Pampa La Bola and San Pedro de Atacama (during February 27–March 15, April 5, and October 26–November 2, 2002), Nobeyama (during February 13 and August 11–13, 2002), and Mitaka (during February 6–22, June 19, and July 26–August 9, 2002, and March 20–21, 2003).

2.3 Satellite data

Global distribution of the UV intensity was evaluated with archived data of the Earth Probe (EP)/Total Ozone Mapping Spectrometer (TOMS) [7]. The TOMS instrument is a second-generation backscatter ultraviolet ozone sounder. TOMS measured the total column density of ozone under all daytime observing and geophysical conditions by observing both incoming solar energy and backscattered UV radiation at six wavelengths. Backscattered radiation is solar radiation that has penetrated to the Earth's lower atmosphere and is then scattered by air molecules and clouds back through the stratosphere to the satellite sensors. Along that path, a fraction of the UV is absorbed by ozone. By comparing the amount of backscattered radiation to observations of incoming solar energy at identical wavelengths, one can calculate the Earth's albedo. Changes in albedo at the selected wavelengths can be used to derive the amount of ozone above the surface.

TOMS made 35 measurements every 8 s, each covering 50–200 km wide on the ground, strung along a line perpendicular to the motion of the satellite. Due to the nature of the platform's orbits, the high northern latitudes were not completely covered during the Antarctic ozone hole season. Almost 200,000 daily measurements covered every single spot on the Earth except areas near one of the poles, where the Sun remains close to or below the horizon during the entire 24 hr period. Near-real time total column ozone abundances were provided at a $1^\circ \times 1.25^\circ$ latitude/longitude resolution. Due to the resolution discrepancy between the gridded elevation and ozone datasets, every fifth $1^\circ \times 1^\circ$ grid cell centroid fell on the boundary of two ozone grid cells. In this case the column ozone amount for that cell was taken as the simple average of the two adjoining cells.

Effects of topography on the amount of radiation reaching the surface can be significant. Higher altitude regions will receive more direct beam radiation than will lower altitude regions since the number of scattering events decrease with the density of the atmosphere, resulting in less radiation being scattered back to space. Rand's global elevation and depth dataset obtained from the National Center for Atmospheric Research (NCAR) Data Support Section was used to scale surface-level UV dose calculations at each grid cell. A nominal scaling factor of 6% increase per kilometer change in altitude was employed to estimate exposure levels for areas above sea level.

3 Global distribution of UV Index

Presented in Figure 3 is a collection of archived images of the global distribution of UV Index (UVI)[3] on the first day of the month from 2000 October to 2001 September, generated at a $1^\circ \times 1^\circ$

[2]UV Index (UVI) is calculated by weighting the UV irradiances by the Erythemal Response Spectrum and integrating them over the 290 to 400 nm range and multiplying them by $0.4\,(\mathrm{W\,cm^{-2}})^{-1}$.

[3]The UVI scale calculated in these images is the index defined by the World Meteorological Organization (WMO). This value is calculated by finding the instantaneous erythemal UV exposure value at local noon (measured in $\mathrm{W\,cm^{-2}}$) and scaling this value by a factor of 0.4. This procedure will typically result in values ranging

latitude/longitude resolution using near-real time total column ozone abundances measured by EP/TOMS [8]. These estimates represent clear-sky values for these dose variables, and cloud cover is not incorporated into the model due to the lack of a corresponding global gridded cloud cover data available in near-real time. As a result, these values represent the maximum potential UVI and daily integrated erythemal dose for the day, and the presence of cloud cover, excessive airborne particulates and/or ground-level ozone would reduce these values. Note, however, that even under partly cloudy skies, the UVI can reach its maximum value if the Sun appears between clouds and direct sunlight reaches the Earth's surface.

There are several factors that control UVI, and their effects are visible in the spatial UVI distribution shown in Figure 3. The first one is the airmass and it appears in the latitudinal difference and the seasonal variation of the UVI distribution. Northern part of Chile is outstanding in this figure. UVI is the world's highest in northern Chile, with the second highest in Himalayan heights. Located near the tropic of Capricorn, UVI comparable to or exceeding 20 is expected in northern Chile at local noon from November to March. UVI in northern Chile is the lowest in June–July but even during that period the value at local noon exceeds 8 (high).

The other factor that control UVI is the UV opacity. The UVB opacity is known affected by total ozone column density. Clouds, air pollution, haze and elevation also have affects on the amount of UV radiation reaching the surface. Because the effects of cloud cover, air pollution and haze are not included in the model calculation, however, only effects of ozone column and elevation are reflected in the spatial distribution. We will touch the effects of the cloud cover in Section 4.3.

4 UV opacity

4.1 UVA opacity

Shown in Figure 4 is variation of the UVA intensity toward three positions of the sky — toward the Sun ($I^{+}_{\rm sun}$), toward the zenith ($I^{+}_{\rm zen}$), and toward the horizon ($I_{\rm hor}$) — as a function of the elevation of the Sun. Solar-elevation dependent variation of the values toward the zenith is mostly explained by the incident angle dependence of the sensor (Figure 5).

The extinction curve as a function of the airmass was plotted in Figure 6 for the five sites. The UVA opacity was estimated by fitting the airmass dependence of the logarithmic intensity corrected for the contamination of the extended component, and the typical opacity was about 0.4 at Pampa La Bola (alt. = 4800 m), about 0.6 both at San Pedro de Atacama (alt. = 2450 m) and at Nobeyama (alt. = 1350 m), and about 0.7 at Mitaka (alt. = 60 m, under best conditions), respectively.

4.2 UV Index and UVB opacity

UV Index (UVI) was measured in the same manner and was used to estimate the UVB opacity. Unlike the measurements of UVA intensity, the measurements of UVI with SafeSun suffered from severe effects of quantization. The measured UVI at Mitaka and Nobeyama during winter, for example, ranged only from 0 to 2, and was comparable with the minimum readout of the instrument, whereas the UVA intensity ranged from 0 to 1.4 with a resolution of 0.01 to give a dynamic range of the observations of 140.

from 0–15 in mid-latitudes. Tropical regions will experience indexes greater than 15, with extremely high values greater than 20 often occurring in high altitude regions. The daily integrated erythemal dose is found by estimating the instantaneous dose values at every half hour during the day, and summing these values over the course of the day using a simple trapezoidal numerical integration scheme. When summed over time, the instantaneous values calculated in watts per square centimeter are then given in $\mathrm{kJ\,m^{-2}}$, the total amount of radiant energy received over a $1\,\mathrm{m^2}$ area during the daytime.

As shown in Figure 7, the maximum UVI were 14 at Pampa La Bola, 12 at San Pedro de Atacama, whereas at Mitaka it was 9 in summer and only 2 in winter. Again, solar-elevation dependent variation of the values toward the zenith is mostly explained by the incident angle dependence of the sensor (Figure 8), which is close to the cosine response.

The extinction curve as a function of the airmass was plotted in Figure 9 for the four sites. Despite the instrumental limitations an outstanding difference of UVB opacity was found among the sites. Typical UVB opacity was about 1.4 at Pampa La Bola near the AOS site, while it was about 1.8 both at San Pedro de Atacama near the OSF site and at Nobeyama, and about 2.0 at Mitaka (best conditions), respectively.

As for the prediction and monitoring, daily UVI in major Chilean cities (e.g., Santiago and Antofagasta) is available from Red Nacional de Medición Ultravioleta homepage [9], and values for Antofagasta reasonably agreed to the measured ones at the AOS and OSF sites. Hence this prediction website may be useful for evaluation of potential risks of UV exposure at the AOS and OSF sites.

4.3 Effects of weather conditions

As shown in Figures 4 and 7, the UV intensity sometimes scatters. This is explained by variation of weather conditions that affects UV opacity. The transmission used in the National Centers for Environmental Prediction (NCEP) forecast models are that: clear skies allow 100% transmission of UV radiation to the surface, scattered cloud conditions allow 89% transmission, broken cloud conditions allow 73%, and overcast cloud conditions allow 32% transmission. Note however attenuation in the ultraviolet region are not as great as those of total intensity, since water in clouds attenuates solar infrared much more than UV (e.g., Diffey 1980). The risk of overexposure may be increased under these conditions because the warning sensation of heat is diminished.

Light clouds scattered over a blue sky make little difference to UV intensity unless directly covering the Sun, while complete light cloud cover reduces terrestrial UV to about one half of that from a clear sky. Even with heavy cloud cover the scattered ultraviolet component of sunlight (often called skylight) is seldom less than 10% of that under clear sky (Paltridge & Barton 1978).

4.4 Ground reflection

The effects of ground reflection was evaluated by measuring the UVA intensity toward the ground, which was about 2.5% of the value toward the Sun at Pampa La Bola and about 4.5% at San Pedro de Atacama, respectively. A significant variation in ground reflectivity was observed when there was snow cover. The UVA intensity and the UV Index measured toward the snow-covered ground were 0.43 and 4, respectively, and corresponded to 81% and $\sim 60\%$ of the values toward the zenith. When we focus on scattered UV, the contribution of the scattered component from snow-covered ground exceeded that from a blue sky.

5 UV dose at the site and implication to site safety

5.1 UV dose at the site

One might think the above difference in UV opacity is relatively small if one simply focus on the peak UV intensity around noon during summer. However, the effect appears more severely in annual doze that integrates the UV intensity over the daytime and over the year. There are several factors that contribute to extremely high UV dose near the AOS: low UV opacity, large total hours of sunshine, low latitude, and high ground reflectivity.

As shown in Figure 10 that plots UVA intensity and UV Index measured toward the Sun as a function of time of the day, the daily UV dose at the ALMA site is several times larger than that at Mitaka under excellent weather. The difference is even severer in UVB. Note that the data were taken when the weather was good enough and thus the values at Nobeyama and Mitaka is usually much less, because of less hours of sunshine. Because of the low latitude, seasonal difference of the daily UV doses at the ALMA site seem small compared to the ones in Japan. Namely, the UV dose at the ALMA site can be unusually large throughout the year unless special cares are taken.

5.2 Effects of UV dose to human health

The effects of UV dose to human health have been extensively studied with particular interest in damages of skin and eyes.

As far as is known [e.g., 1, 2, 3], acute exposure of skin to intense UV causes sunburn and chronic exposure results in loss of elasticity and increased aging. Some individuals, usually those living in areas with limited sunlight and long dark winters, may also suffer severe photo-allergies to the UVB in sunlight. Increased absorption of UVB triggers a thickening of the superficial skin layers and an increase in skin pigmentation, which act to protect the skin against future sunburns.

This protective mechanism also makes the skin more vulnerable to skin cancer, however. There are various types of skin cancer. One main class is cutaneous melanomas, the cancers of the pigment cells. The other main types are basal cell carcinomas and squamous cell carcinomas, cancers of the epithelial cells. These carcinomas of the skin are sometimes, collectively, called non-melanoma skin cancers. In white Caucasians (Skin Type II–III of Table 1), the incidence of these cancers ranks high among the various types of cancer. The incidence is lower in more pigmented populations, typically by a factor of 10 or even 100. The mortality rate is low in comparison with that for other types of cancer: approximately 1% in areas with good medical care. The non-melanoma skin cancers are clearly correlated to sunlight. They occur mostly in light-skinned people, and then predominantly on skin areas most exposed to sunlight, such as the face. In people of comparable genetic background, the incidences are higher in the sunnier geographical areas.

The eye is also directly accessible to solar UV radiation. One of the adverse effects caused by UV radiation in the eyes is snow blindness. It occurs typically when the eyes are exposed to UV radiation coming from unusual directions, such as in snow-covered mountains. Snow blindness is very painful, sometimes described as the feeling of having sandpaper in the eyes. It usually starts several hours after exposure and gives the victim a very uncomfortable night; the pain may even last several days, depending on the severity. The eyes usually heal spontaneously. The medical name for the condition is photokeratitis. It is an acute inflammation of the superficial layers of the eye, the cornea and conjunctiva. The effect is dose related, and in severe cases there may be lasting damage. The eye has no adaptation against this effect; the eye even tends to become more sensitive to the next exposure. Within the solar spectrum, the most effective wavelengths are in the UVB range. Although the eyes may be protected by UV-absorbing sunglasses, snow blindness is a frequently occurring problem. There is little doubt that increased solar UVB irradiance, with unchanged behavior, will lead to increased incidence and severity of snow blindness.

Another possible effects on eyes are cataracts, which are opacities in the lens of the eye which impair vision. Cataracts occur mainly in elderly people and may ultimately lead to blindness. It is becoming increasingly clear that sunlight, among other factors, plays a role in the formation of cataracts. Ophthalmologists distinguish three main types of cataract: nuclear cataract, which occurs in the nucleus of the lens; cortical cataract, which occurs in the surrounding cortex;

and posterior subcapsular cataract, which occurs beneath the posterior capsule of the lens. An association with sunlight was reported by several researchers. In some of the epidemiological studies, the UV radiation in sunlight is stated to be responsible. It is questionable whether the methods followed in epidemiological studies have the resolving power to reach such a conclusion. A predominant role of UVB radiation is, however, supported by data from animal experiments.

Although UV provides a physiological benefit by inducing vitamin D production in the skin, vitamin D is readily obtained in developed countries from a number of dietary sources and its cutaneous synthesis should not be the principle concern driving medical recommendations about UV exposure.

5.3 Recommended protective action

Appropriate protective action is certainly required at the ALMA site. Beside restricting hours spent outdoors, use of a sunscreen and protective wear (e.g., sunglasses and hats) is the first recommended action. Needed types of sunscreen depends on individuals' skin types, prospected hours to be spent outdoors, and the UV Index of the day.

Here are some of the tips and recommendations by experts (e.g., [10]):

Exposure control

- Prevent unnecessary exposure to UV (see, Table 2 for the minutes to skin damage for different skin types).
- Seek shade as much as possible while outside.
- Avoid prolonged exposures near reflective surfaces (e.g., ground covered with snow, sand, or salt).
- Well prepared during daytime regardless of the weather and the time of the day. It is because UV intensity is significant even when elevation of the Sun is not very high because of low UV opacity, and thus will have serious impact on vertically standing surfaces like human faces. General idea that "If your shadow is longer than your are tall, it is okay to be outside." is not appropriate at the ALMA site.
- Discourage use of tanning parlors. Tanning devices can damage the skin and eyes as much as direct sunlight and have been linked to increased risk of developing melanoma.
- Some medications can increase UV sensitivity (see, Table 3). Certain antibiotics, birth control pills, diuretics, antihistamines and antidepressants may cause increased sensitivity to the Sun. Take extra precautions if you are taking any of these medications.

Sunscreen

- Use a sunscreen every day of the year. As shown in Section 4.3, the UVB intensity attenuation is not much as we feel from that of visible sunlight.
- Wear a sunscreen that has at least a Sun Protection Factor (SPF) of 15, because a sunscreen with SPF 8 filters out only 86% of damaging UV, whereas that with SPF 15 and 30 blocks 92% and 96% of it, respectively.
- Apply to dry skin about 15 to 30 minutes before going outdoors.
- Use plenty. Studies have shown that the average person uses about half the amount of sunscreen that the manufacturer used when determining the SPF value.

- Remember apply sunscreen to lips, ears and exposed scalp.
- Reapply after sweating, swimming or toweling off.

Protective clothing

- Dress accordingly. Choose clothes that cover the arms, legs and neck. Go for long sleeves, collars, long pants or skirts. Dark colors are better at absorbing UV than light colors.
- Wear hats. A hat brim of 10 cm or greater is recommended. Make certain that the top and brim of a straw hat have sunproof liners in place.

Eyewear

- Wear protective eyewear. Sunglasses with UV-blocking filters are very important.
- Because of the high reflectivity of the ground, sunglasses that entirely cover the eyes will be preferable to avoid snow blindness due to reflected UV from the ground, and will be definitely needed when large fraction of the ground is covered by snow.

Workplace strategy

- Use UV protective glass for windows. Sky windows with normal glass can transmit up to 50% of total incident UV.
- Do not rely too much on shade. Feeling cool under shade can give a false sense of security that we are not getting an UV dose. Even without direct illumination by the Sun, one can badly sunburnt by reflected and scattered UV.
- Avoid setting reflective material at low elevation.

5.4 An example of site safety policy

Enhanced occupational exposure of outdoor workers to intense solar UV is understood to be occupational hazard. In the United States, OSHA general standards section 1910.132 (a) requires employers to provide protective equipment to employees. The ALMA project may also follow this kind of occupational safety standards. To ensure that the risk of adverse health effects due to solar UV radiation is minimized, it may be natural to have a site safety policy on this issue. For example, following items [12] may be worth considered:

- Assessment of the potential for occupational exposure to solar UV radiation among employees engaged in outdoor work and identification of potentially at risk personnel.
- Provision and maintenance of suitable and protective clothing for potentially at risk personnel.
- Provision and maintenance of stocks of sunscreens for potentially at risk personnel.
- Education and training of at risk personnel on the effects of UV exposure, use of protective clothing and sunscreens.

6 Future works

It is obviously important to measure the UV intensity at the sites with a UV spectro-radiometer with appropriate angular response. Seasonal variation is also to be examined. The UVB dose during austral spring is of the largest interest, because the ozone hole has been measured to be the largest in this season. Furthermore, reference data at Socorro VLA site (alt. = 2120 m), where the ALMA prototype antennas will be tested and where we have experiences of operating a large array, will be needed.

7 Summary

UV intensity near the AOS and OSF sites in northern Chile was measured with handheld UVA and UVB radiometers and was compared with that taken at Socorro AOC, Nobeyama, and Mitaka.

Typical UVA opacity was about 0.4 at Pampa La Bola near the AOS site, about 0.6 both at San Pedro de Atacama near the OSF site and at Nobeyama, and about 0.7 at Mitaka (best conditions), respectively. The UVA intensity toward the Sun measured at Pampa La Bola near the sunset (elevation $\sim 20°$) was still comparable with the highest value recorded at Mitaka.

The difference becomes even more outstanding in UVB. The UV Index, which chiefly reflects UVB intensity, measured with a handheld UVB radiometer was in reasonable agreement with that predicted with the satellite data, and both consistently indicate that the UVB is extremely high at the AOS and OSF sites. The UV Index typically exceeded 7 (high) for 6 hours near the AOS site.

Effects of UV dose and recommended protective action were summarized from a number of literatures, and an example of site safety policy was proposed.

We thank Satoshi Yamamoto for providing us with the UVA sensor.

References

[1] Diffey, B. L. 1991, "Solar Ultraviolet Radiation Effects on Biological Systems," Physics in Medicine and Biology, 36, 299
(available at `http://www.ciesin.org/docs/001-503/001-503.html`)

[2] van der Leun, J. C., & de Gruijl, F. R. 1993, "Influences of Ozone Depletion on Human and Animal Health," in UVB radiation and ozone depletion: Effects on humans, animals, plants, microorganisms, and materials, ed. M. Tevini, 95 (Boca Raton: Lewis Publishers)
(available at `http://www.ciesin.org/docs/001-540/001-540.html`)

[3] United Nations Environment Programme 1998, "Environmental Effects of Ozone Depletion: 1998 Assessment"
(available at `http://sedac.ciesin.org/ozone/docs/UNEP98/UNEP98.html`)

[4] Yamamoto, S., & Oka, T. 2000, "Measurements of Ground Resistance and UV Field at ASTE/LMSA/ALMA Sites," LMSA Memo 2000-011 [text in Japanese]

[5] `http://www.srrb.noaa.gov/highlights/sunrise/azel.html`

[6] `http://www.safesun.com/`

[7] `http://toms.gsfc.nasa.gov/`

[8] `http://sedac.ciesin.org/ozone/maps/archive.shtml`

[9] `http://www.indiceuv.cl/home.htm`

[10] McKinlay, A. F., Driscoll, C. M. H., Meara, J. R., Pearson, A. J., Saunders, R. D., & Stather, J. W. 2002, "Advice on Protection Against Ultraviolet Radiation," Documents of NRPB, 13
(available at `http://www.nrpb.org/`)

[11] Allen, J. E. 1993, "Drug-induced Photosensitivity," Clinical Pharmacy, 12, 580

[12] University College Australian Defense Force Academy 2001, "Protection of Outdoor Workers Exposed to Ultraviolet Radiation from Sunlight"
(available at `http://www.unsw.adfa.edu.au/`)

Table 1: Skin type determination characteristics

Skin type	I	II	III	IV	V	VI
Skin color	alabaster	white	pale brown	olive brown	brown	black
Eye color	light blue, green	blue, gray	blue, hazel	brown	dark brown	black
Hair color	reddish	fair, blonde	chestnut, brown	brown	dark brown	black
Freckles	Yes	some	No	No	No	No
Burns	always	usually	sometimes	rarely	never	never
Peels	always	usually	sometimes	rarely	never	never
Blisters	always	usually	sometimes	rarely	easily	never
Tans	never	weakly	good	very good	always	
Race	English	European	European	Asian, South American	Hispanic, East Indian	African American

Table 2: UV Index (UVI) and minutes to burn for deferent skin types

Exposure category	UVI	Minutes to burn for various skin types					
		I	II	III	IV	V	VI
Minimal	0, 1, 2	> 60	> 60	> 60	—	—	—
Low	3, 4	45	50	60	120	—	—
Moderate	5, 6	30	40	50	100	—	—
High	7, 8, 9	20	30	40	80	120	—
Very high	> 10	< 15	< 20	< 30	< 60	< 100	< 120

[6].

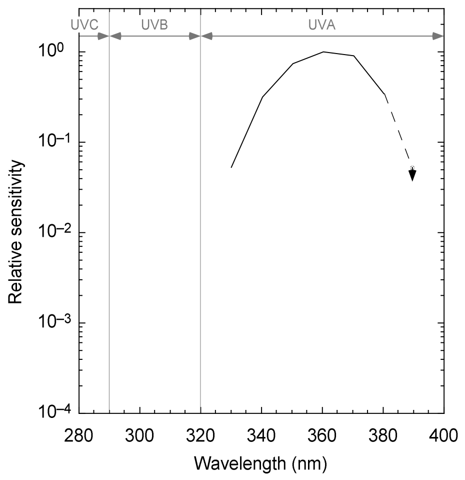

Figure 1: Typical relative spectral sensitivity of Ushio UVD-365PD sensor (Ushio Inc. 2001, private communication).

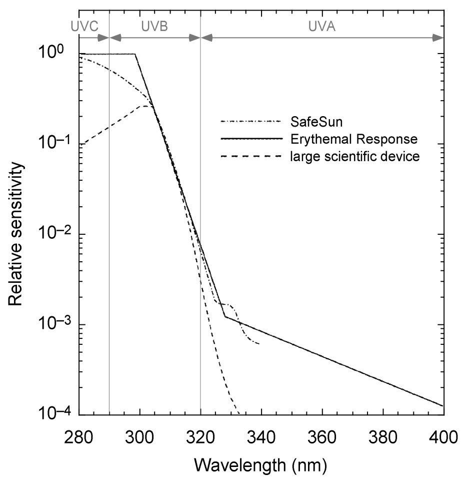

Figure 2: Relative spectral sensitivities (normalized at 310 nm) of SafeSun Classic personal UV radiometer (*dot-dash line*) and a large scientific device widely used for laboratory/meteorological measurements (*dashed line*) overlaid on the Erythemal Response Spectrum pattern (*solid line*) [6].

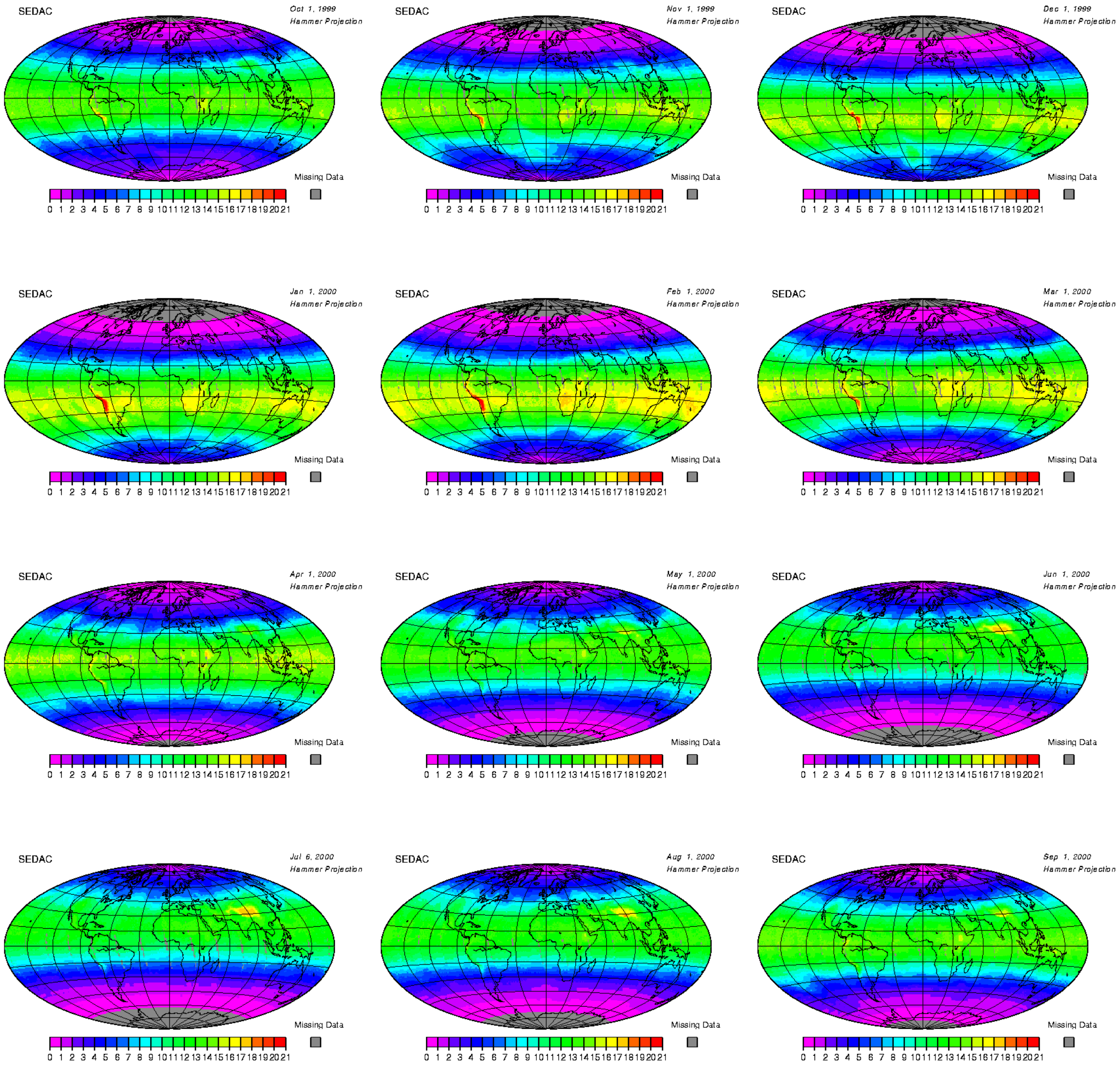

Figure 3: Global distribution of local noon estimates of the UV Index (UVI) on the first day of the month from 2000 October to 2001 September, generated at a $1^\circ \times 1^\circ$ latitude/longitude resolution using near-real time total column ozone abundances measured by NASA's Total Ozone Mapping Spectrometer (TOMS) carried on board the Earth Probe satellite platform. Note the effects of cloud cover has not been incorporated. The projection is an equal area Hammer-Aitoff projection.

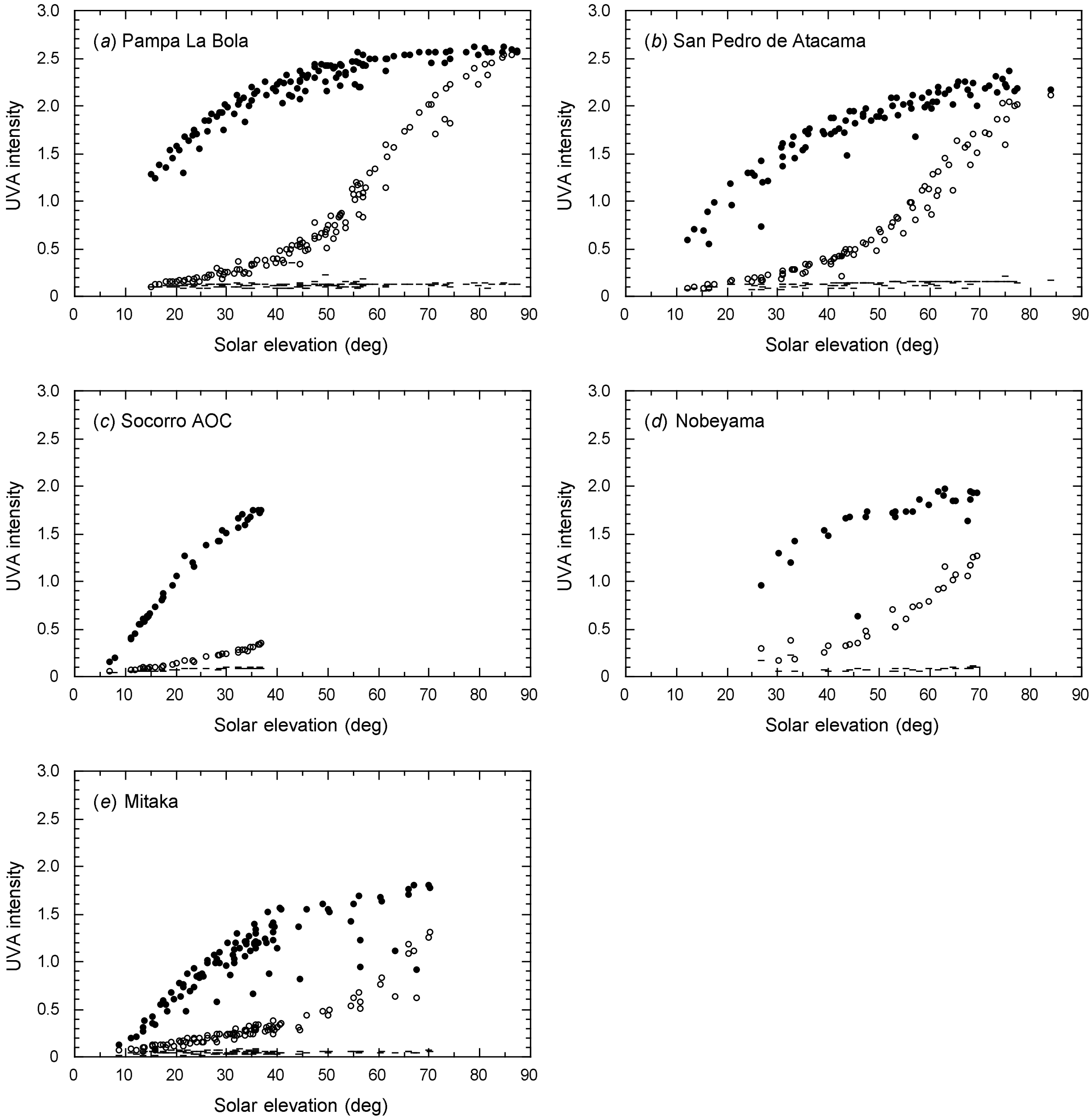

Figure 4: Solar elevation dependence of UVA intensity toward three positions of the sky — toward the Sun ($I^{+}_{\rm sun}$; *filled circles*), toward the zenith ($I^{+}_{\rm zen}$; *open circles*), and toward the horizon in the opposite direction to the Sun ($I_{\rm hor}$; *dashes*) — measured at (a) Pampa La Bola, (b) San Pedro de Atacama, (c) Socorro AOC, (d) Nobeyama, and (e) Mitaka. The absolute values of the UVA intensity are readouts of the sensor and should be taken as arbitrary, while their relative scaling is accurate.

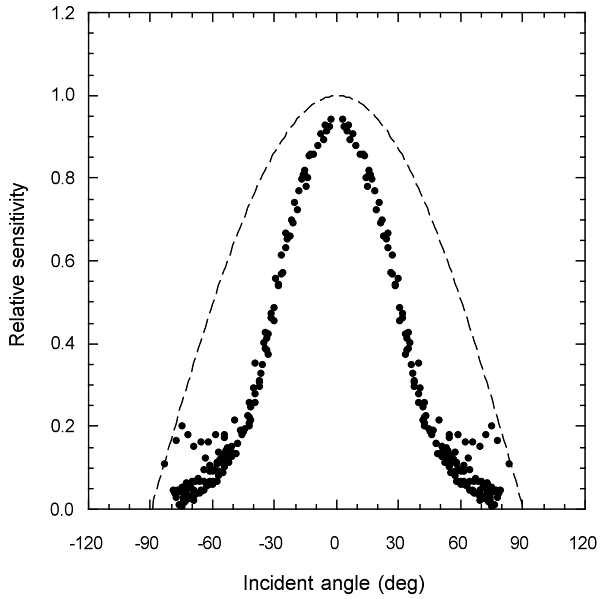

Figure 5: Incident angle dependence of the UVD-365PD sensor measured toward the Sun. Dashed line corresponds to the cosine response.

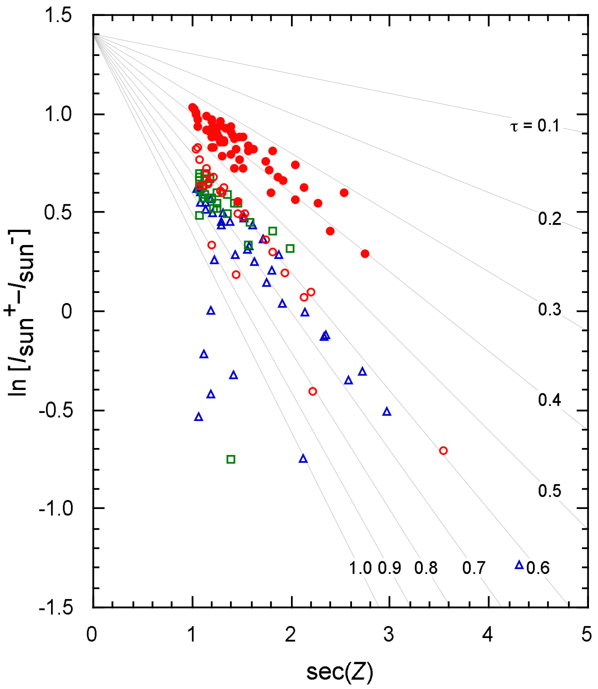

Figure 6: Airmass dependence of the UVA intensity toward the Sun, measured at Pampa La Bola (*red filled circles*), San Pedro de Atacama (*red open circles*), Socorro AOC (*blue filled squares*), Nobeyama (*green open squares*), and Mitaka (*blue open triangles*), subtracted for uniform component. Thin lines indicate extinction curves with an intersection at $\ln(I^{+}_{\rm sun} - I^{-}_{\rm sun}) = 1.4$.

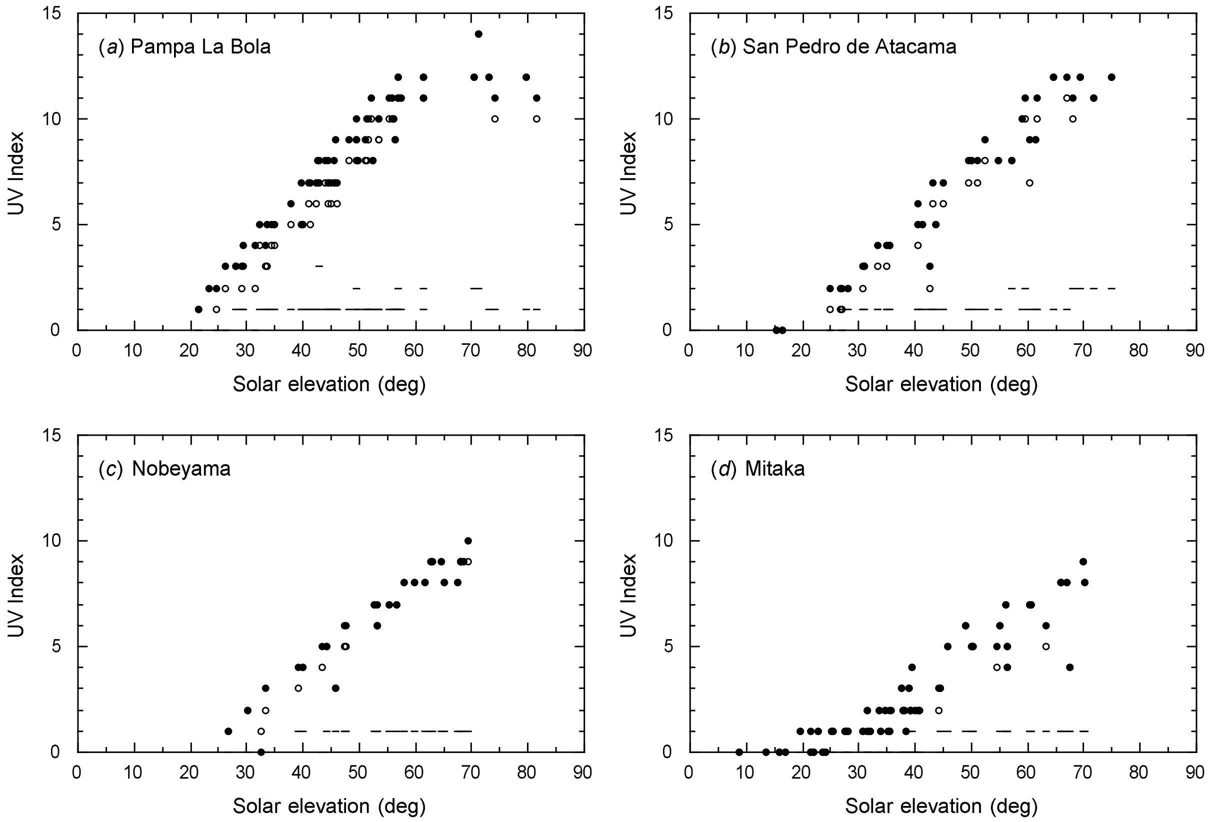

Figure 7: Solar elevation dependence of UV Index, which chiefly reflects UVB intensity, toward three positions of the sky — toward the Sun ($I^{+}_{\rm sun}$; *filled circles*), toward the zenith ($I^{+}_{\rm zen}$; *open circles*), and toward the horizon in the opposite direction to the Sun ($I^{+}_{\rm hor}$; *dashes*) — measured at (*a*) Pampa La Bola, (*b*) San Pedro de Atacama, (*c*) Nobeyama, and (*d*) Mitaka.

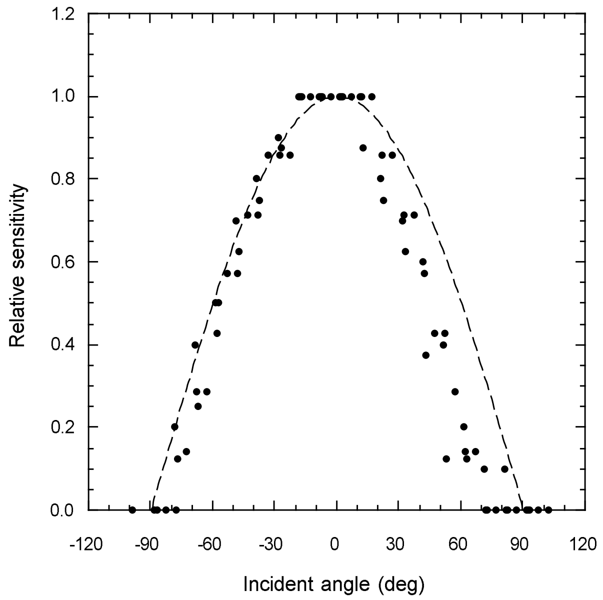

Figure 8: Measured incident angle dependence of SafeSun. Dashed line corresponds to the cosine response. Incident angle is positive toward the foreside of the observer.

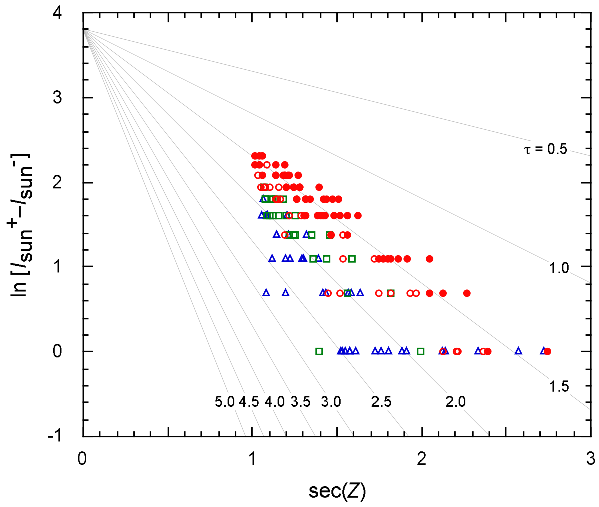

Figure 9: Airmass dependence of the UV Index, which chiefly reflects UVB intensity, toward the Sun, measured at Pampa La Bola (*red filled circles*), San Pedro de Atacama (*red open circles*), Nobeyama (*green open squares*), and Mitaka (*blue open triangles*), subtracted for uniform component. Thin lines indicate extinction curves with an intersection at $\ln(I_{\rm sun}^{+} - I_{\rm sun}^{-}) = 3.8$.

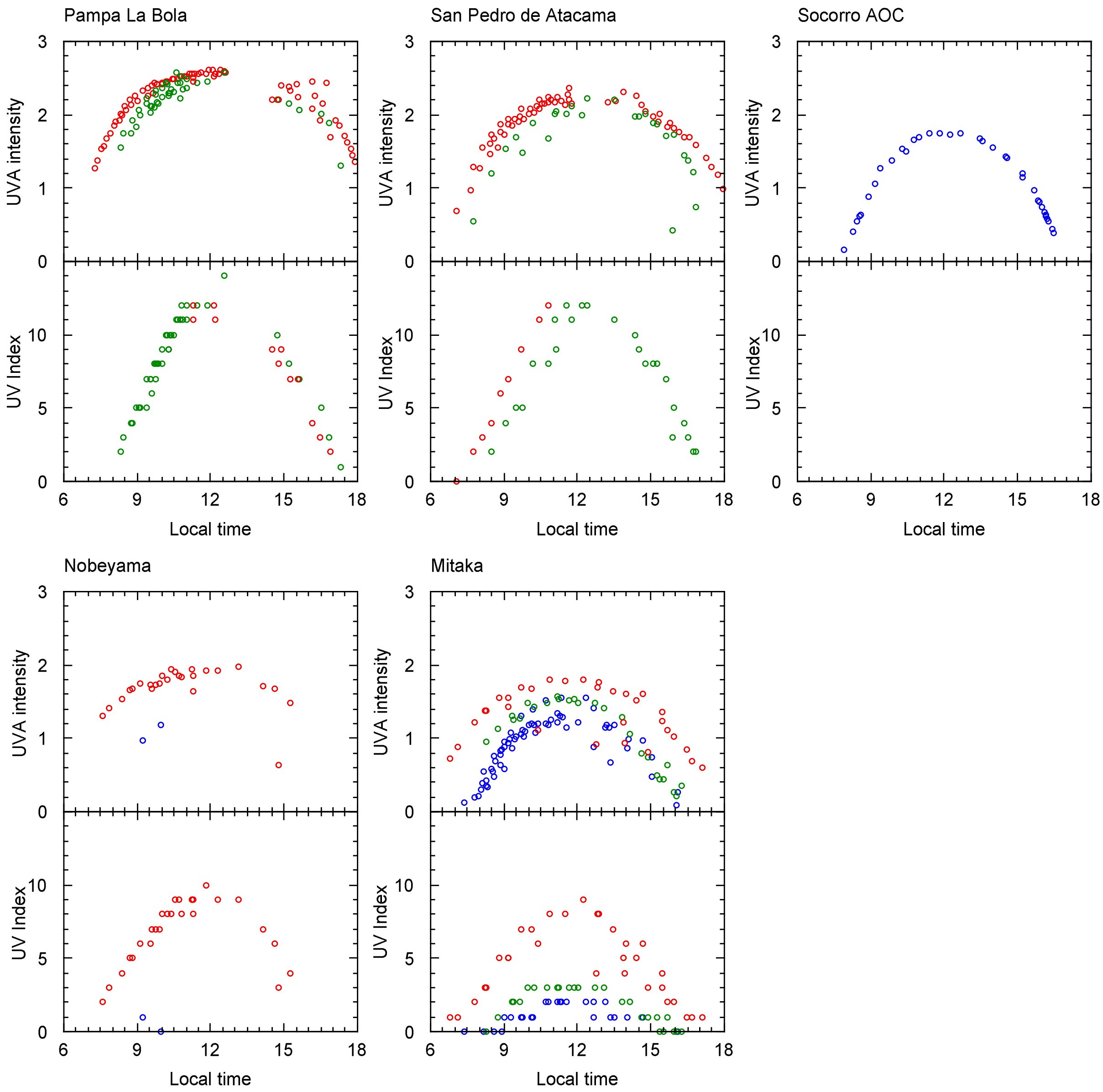

Figure 10: UVA intensity (arbitrary unit) and UV Index, which chiefly reflects UVB intensity, measured toward the Sun as a function of local time of day (without daylight saving time correction). Red, green, and blue symbols denote data points taken during local summer (November–February in Chile, and May–August in the northern hemisphere), spring and autumn (September–October, March–April), and winter, respectively. Note that the data were taken when the weather was good enough and thus the values at Nobeyama and Mitaka is usually much less because of smaller probability of fine weather.

Table 3: Drugs associated with photosensitivity reactions [11]

Category	Drugs
Anti-infectives	amantadine
	lomefloxacin, enoxacin, naldixic acid, ofoxacin, ciprofloxacin
	sulfisoxazone, trimethoprim
	democlocycline, doxycycline
	chloroquine, pyrimethamine
	griseofulvin, dapsone, pyrazinamide
Anti-inflammatory	desoximetasone, hydrocortisone
	ibuprofen, piroxicam
Cardiovascular	amiodarone, quinidine
	diltiazem, nifidipine
	hydrochlorothiazide, triamterene
CNS agents	carbamazepine, clomipramine
	alprazolam, chlordiazepoxide
	chlorpromazine, thioridazine
Miscellaneous	glyburide, chlorpropamide, tolbutamide, diphenhydramine
	methotrexate, vinblastine, dacarbazine, flourouracil
	etretinate, isotretinoin
Topical agents	tretinoin, coal tar, benzoyl peroxide
Other misc. agents	gold salts, minoxidil, psoralens